

1 **AUTHOR INFORMATION AND QUALIFICATIONS**

2 **Dr Lewis E. MacKenzie, Ph.D.**^[a].

3 **Professor Andy R. Harvey, Ph.D.**^[b]

4 **Professor Andrew I. McNaught, MD, FRCOphth.**^[c,d].

5 [a] Research Fellow. School of Biomedical Sciences, Faculty of Biosciences, University of Leeds, United
6 Kingdom, LS2 9JT.

7 [b] Professor of Optics. School of Physics and Astronomy, University of Glasgow, United Kingdom. G12
8 8QQ.

9 [c] Consultant Ophthalmologist. Department of Ophthalmology, Cheltenham General Hospital,
10 Gloucestershire Hospitals NHS Foundation Trust, Gloucestershire, United Kingdom, GL53 7AN.

11 [d] Honorary Professor. School of Health Professions, Plymouth University, Plymouth, United
12 Kingdom, PL4 8AA.

13
14 Corresponding author: Andrew I. McNaught

15 Email: andy.mcnaught@btopenworld.com

16 Telephone: 0124-227-2527

17

18 Spectroscopic oximetry in the eye: a review

19 ABSTRACT

20 **Introduction:** Non-invasive measurement of blood oxygen saturation via spectroscopic imaging has
21 facilitated insights into the development and progression of a variety of ocular conditions, including
22 retinal vascular occlusion, diabetic retinopathy and glaucoma. Major developments since the late 90s
23 have been enabled by advancements in imaging technology, computational image analysis, and
24 experimental methods.

25 **Areas covered:** We review the theory of spectroscopic oximetry, the ocular blood vessels targeted for
26 oximetry, imaging systems used for oximetry, and oximetry validation methods. Important
27 physiological and clinical insights provided by oximetry in the eye are detailed.

28 **Expert commentary:** Oximetry has revealed physiological norms and auto-regulatory effects in the
29 retina, choroid, episcleral, and bulbar conjunctival blood vessels. Retinal oximetry has provided crucial
30 insight into the development of diabetic retinopathy and glaucoma, and has enhanced the evaluation
31 and treatment of retinal vessel occlusion. Commercially available retinal oximetry systems have
32 enabled oximetry in the clinic. The development more sophisticated phantoms that resemble *in vivo*
33 environments has oximetry validation in diverse oximetry applications. New insights into ocular
34 physiology and disease are likely to be gleaned from future studies.

35 -----

36 **Keywords:** oximetry, retina, autoregulation, diabetes, glaucoma, vessel occlusion, choroid, bulbar
37 conjunctiva.

38

39 1. INTRODUCTION

40 Oximetry - the measurement of blood oxygen saturation (OS) – can be achieved non-invasively by
41 measuring the spectrum of light absorbed by blood. This is achieved by imaging the eye at two or more
42 wavelengths of light, and calibrating the OS to absorption of light by either (1) assuming standard
43 normal OS values or (2), by combining information from many wavelengths into a sophisticated
44 physical model incorporating the known spectral properties of blood with other biological and optical
45 parameters.

46 Since the late 1950s, retinal oximetry has progressed from a photographic technique [1–3] through
47 to the cutting edge of digital imaging technology with automated computational analysis.[4,5] Over
48 the decades, retinal oximetry has revealed valuable insights into retinal physiology and metabolism
49 under conditions such as flicker illumination,[6,7] dark adaptation,[8] hyperoxia,[4,9,10] and acute
50 mild hypoxia.[11,12] Further, retinal oximetry has provided insights into the development and
51 progression of ocular diseases such as diabetic retinopathy,[13–17] glaucoma,[18–22] and retinal
52 vessel occlusion.[23–26] Recently, oximetry has allowed the understanding of the fundamental
53 physiological oxygen dynamics of the bulbar conjunctival circulation,[27] the episcleral vessels,[27]
54 and the choroidal circulation.[28]

55 From a patient's perspective, the experience of oximetry imaging in the eye is typically
56 indistinguishable from conventional retinal-fundus imaging because oximetry systems are typically
57 based on a modified conventional retinal-fundus cameras[4,11,16] or multi-wavelength scanning laser
58 ophthalmoscopes.[10,29] As such, a great deal of oximetry innovation has arisen from improved
59 image recording, computational image analysis, and the development of complimentary functional
60 oxygen-sensitive stress interventions that allow insight into OS under altered metabolic conditions.
61 These intervention tests include subjecting subjects to hyperoxia,[6,7] acute mild hypoxia,[11,12] or
62 altered light-exposure conditions.[6–8] As well as physiological and clinical insights, these intervention
63 tests help validate the accuracy of oximetry measurements.

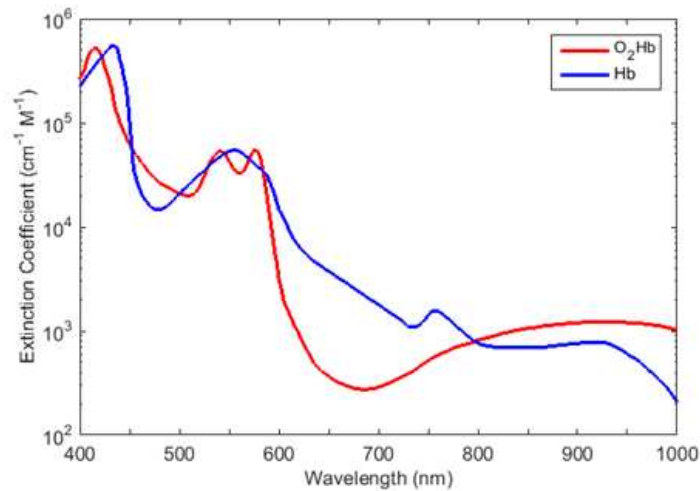
64 Invariably, advances in oximetric-imaging technology have provided new insights and applications.
65 In particular, the development of commercially available retinal oximetry devices with automated
66 analysis – such as the *Oxymap T1* (Oxymap ehf, Iceland) [4] and *Imedos* (Imedos Systems UG,
67 Germany)[16] retinal oximetry systems - have enabled oximetry in the clinic, allowing insights into
68 treatment of individual patients[24] and also enabling clinicians to build large datasets with high
69 statistical power. Additionally, the development of oximetry systems with capability for imaging with
70 greater temporal[11] and spatial resolution[29] enable development of novel techniques and fresh
71 insights by investigating OS of smaller blood vessels or by studying OS dynamics on a shorter timescale.
72 For example, snapshot multispectral imaging technology has enabled measurement of rapid oxygen
73 diffusion in the bulbar conjunctiva[27] and adaptive optics have enabled oximetry in small retinal
74 vessels, which are not typically studied due to their small diameters.[29]

75 This review focuses on the current technology and methods of spectroscopic oximetry, new
76 applications in spectroscopic oximetry of the eye, and the clinically useful ophthalmological insights
77 that have been consequently enabled.

78 **2. PRINCIPLE OF SPECTROSCOPIC OXIMETRY**

79 Spectroscopic oximetry is enabled by the distinct absorption spectra of oxygenated haemoglobin
80 (O_2Hb) and deoxygenated haemoglobin (Hb) as shown in Figure 1: partial oxygenation results in an
81 absorption spectrum that is a weighted average of these two spectra. This difference in optical
82 absorption can be clearly seen by eye for a low-volume sample of blood: highly oxygenated blood
83 appears bright red to the eye, whereas deoxygenated blood is much darker in appearance. Whilst this
84 difference in optical absorption is readily observed in *ex vivo* blood samples, it is highly challenging to
85 accurately quantify in the complex optical environment of the eye due to the influence of optical
86 scattering[30] and the uncertain absorption of light by variable background pigmentation.[9,31] There
87 are two approaches to spectroscopic oximetry measurement and analysis: two-wavelength oximetry
88 and multi-wavelength oximetry.

89

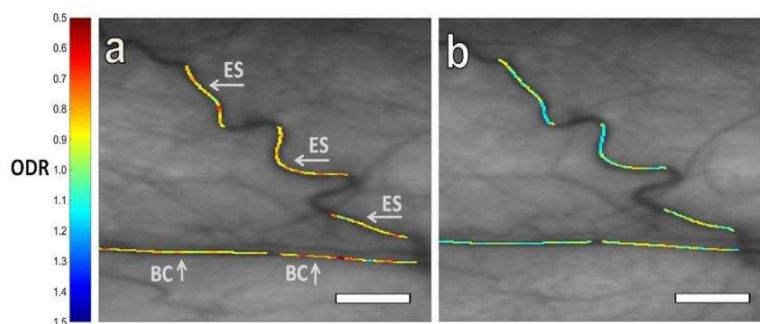


90

91 **Figure 1.** The absorption spectra of oxygenated haemoglobin (O₂Hb) and deoxygenated
 92 haemoglobin (Hb) at visible and near infra-red wavelengths.

93 **2.1. Two-wavelength oximetry**

94 In two-wavelength oximetry, blood vessels are imaged at one OS-sensitive contrast wavelength,
 95 and another – typically OS-insensitive (isobestic) - wavelength. The optical transmission of blood
 96 vessels (T_λ) is measured at each wavelength, and the optical density (OD), defined as: $OD_\lambda =$
 97 $-\log(T_\lambda)$, is computed. From this, the optical density ratio (ODR), defined as $ODR = \frac{OD_{\lambda\text{ contrast}}}{OD_{\lambda\text{ isobestic}}}$, is
 98 calculated. If an isobestic wavelength is used, then for a blood vessel of a given diameter, ODR is
 99 theoretically directly proportional to blood oxygen saturation (verified experimentally in 1959)[1], and
 100 so ODR can be empirically related to OS by measuring ODR of blood vessels at two OS levels followed
 101 by calibration against a blood vessels of known oxygenation (i.e. using pulse oximetry or blood gas
 102 measurement). The theory of two-wavelength oximetry is based upon the simple Beer-Lambert law
 103 of light transmission, which neglects the effects of optical scattering that is incorporated into the
 104 modified Beer-Lambert law.[31] For visualisation purposes, ODR or OS is often overlaid as a colour
 105 map on images of blood vessels (see Figure 2 for an example).[4]



106

107 **Figure 2.** ODR colour-map of bulbar conjunctiva (BC) and episcleral (ES) vessels at (a)
 108 normoxia, and (b) acute mild hypoxia. Reproduced with permission from MacKenzie et
 109 al., (2016).[32]

110 The optimal transmission of a blood vessel for accurate oximetry is around 37%, [33] but, because
 111 the optical transmission of blood vessels varies according to several factors – including vessel

112 diameter - an optical transmission of between 10 % and 70 % has been found to work well.[33] For
113 retinal oximetry, the combination of 570 nm (isobestic) and 600 nm (contrast) wavebands has been
114 commonly adopted for retinal oximetry.[4,11,31] However, the optimal wavelength combinations
115 used for any oximetry study are dependent upon the calibre of vessels of interest and the efficiency
116 of optical imaging and detection systems.

117 Care is required in calibration of two-wavelength oximetry. In early retinal oximetry studies retinal
118 arterial OS was calibrated by comparison with *ex vivo* brachial-artery blood samples and blood gas
119 measurement.[1–3] Whilst useful for establishing relations between retinal arterial OS and systemic
120 arterial OS, *ex vivo* blood gas measurement is undesirable or not feasible and has been rendered
121 unnecessary by the advent of fingertip pulse oximetry which allows non-invasive estimation of
122 systemic arterial OS. However, calibrating arterial OS alone can lead to artefacts in estimated venous
123 OS. For example, it has been shown that ODR is dependent on blood vessel diameter and background
124 pigmentation; so two-wavelength oximetry requires calibration correction factors that are dependent
125 upon both background pigmentation and blood vessel diameter.[9,31] It has recently been postulated
126 that the laminar flow from multiple tributary branching veins, which leads to non-uniform blood
127 oxygenation within a vein may also degrade estimation of OS in retinal veins, which is based upon
128 homogeneous blood oxygenation. This significance of this factor requires experimental testing and
129 validation.[34]

130 Two-wavelength oximetry is the basis for the *Oxymap* and *Imedos* commercial retinal imaging
131 devices which have found considerable use in clinical applications (see Section 6).

132 **2.2. Multispectral oximetry techniques**

133 Multispectral oximetry is broadly defined as any oximetry technique that incorporates information
134 from three or more spectral wavebands to calculate OS.

135 **2.2.1. Three-wavelength oximetry**

136 The simplest form of multispectral oximetry, three-wavelength oximetry, [35] utilises two isobestic
137 wavelengths relatively close to each other on the wavelength spectra combined with a wavelength
138 providing oximetric contrast. From the two isobestic two wavelengths it is possible to quantify the
139 scattering of light by blood, and thus to appropriately alter estimation of blood-vessel transmission
140 via the modified Beer Lambert law.[35] Three-wavelength retinal oximetry was applied to the retinal
141 imaging with a scanning laser device by Delori in the 1980s and 1990s.[36,37] However, three
142 wavelength oximetry was somewhat difficult to apply because of the requirements of three
143 wavebands where blood exhibits similar optical scattering properties; this limited the range of useful
144 wavebands to which it can be applied.[33] As such, three-wavelength oximetry has tended to be
145 superseded by multispectral oximetry using four or more bands.

146 **2.2.2. Multispectral oximetry models**

147 Multispectral oximetry models enable estimation of OS by incorporating the optical transmission
148 of blood at a number of wavebands to isolate the absorption of light by blood and estimate or
149 compensate for other optical parameters, e.g. the scattering of light by blood and tissue, or the optical
150 absorption by melanin pigmentation. Typically, the transmissions of blood vessels are measured and
151 the experimental transmission compared to a theoretical model incorporating these parameters. This
152 enables direct estimation of OS without need of a reference value; i.e. multispectral algorithms are

153 “calibration free”. Thus, multispectral oximetry algorithms can provide quantitative oximetry in blood
154 vessels where OS levels have not yet been measured by other means (e.g. in the spinal cord)[38] or in
155 blood vessels that may be expected to be very different from physiological norms (e.g. studying
156 angiogenesis in tumour development)[39,40]. However, validation of estimated OS from multispectral
157 oximetry algorithms is normally desirable, and provides vital information for the wider field of
158 oximetry (see Section 5).

159 The number of wavebands incorporated into a multispectral imaging system varies greatly. Some
160 oximetry studies incorporate many wavebands (e.g. between 25 and 76 wavebands) into a
161 ‘hyperspectral’ model (see Table 1). Hyperspectral imaging offers the advantage a comprehensive
162 measurement of blood vessel transmission, but as a result of this, hyperspectral imaging systems are
163 typically burdened with a long acquisition time (i.e. > 1 minute) and high data volumes for a single
164 data set. Consequently, challenges arise from subject eye motion and alterations of OS of vessels
165 during hyperspectral measurement. Additionally, some wavebands may be sub-optimal for oximetry;
166 for example, blue wavelengths suffer from lower instrumental signal-to-noise ratios and high
167 absorption by melanin pigmentation, and auto-fluorescence from blood or other tissue. Imaging
168 spectrograph devices offer excellent spectral resolution and have been employed for spectroscopy of
169 the eye,[41] but have only found limited usage because there are no significant advantages associated
170 with over-sampling the absorbance spectra of blood for oximetry.

171 Multispectral oximetry models incorporating a few (typically < 10) key wavelengths have achieved
172 high quality oximetry, whilst reducing acquisition time required for spectral data acquisition. Of
173 particular note is the development of ‘snapshot’ multispectral imaging techniques where several
174 wavebands are acquired simultaneously; this avoids artefacts associated with misregistration of time-
175 sequentially recorded images.[42] The simplest form of snapshot multispectral imaging involves to
176 splitting the imaged light with an optical beam-splitter and then filter each resultant image separately
177 with bandpass filters, or by using a dichroic mirror, [4,42] however, this becomes optically inefficient
178 for large numbers of bands and problematic to implement with a single detector. Several snapshot
179 multispectral imaging devices that require only a single detector have been developed, including use
180 of a lenslet array[43] and the Image Mapping Spectrometer[44] using degmented mirrors; however to
181 date neither of these approaches have been applied extensively to oximetry. A snapshot imaging
182 system which has found significant use for oximetry is the Image Replicating Imaging Spectrometer
183 (IRIS).[11,45] This optically efficient device enables video-rate imaging at eight distinct wavebands
184 optimised for retinal oximetry. The high temporal resolution and 8 wavebands afforded by IRIS has
185 enabled several new oximetry applications, including direct observation of oxygen release by red
186 blood cells.[46]

187
188

Table 1. Retinal oximetry studies utilising multispectral imaging oximetry algorithms.

Study	Wave-range	Known parameters	Estimated parameters	Key reported OS (i.e. normal OS at normoxia - unless otherwise stated)
Schweitzer et al., (1999)[47]	510 – 586 nm 76 wavebands	ϵ , ϵ_{mel}	OS, c, d, η	A: 92.2 ± 4.1 % V: 57.9 ± 9.9 %
Drewes et al., (1999)[48]	629, 678, 821, & 899 nm.	ϵ	OS, S, c, d	A: 101 % V: 65 %
Smith et al., (2000)[49]	488, 635, 670, 752, & 830 nm	ϵ	OS, S, c, d, η	V: 42 - 56 %
Alabboud et al., (2007)[50]	500 – 700 nm 27+ wavebands	ϵ , S	OS, d, c, η	A: 96 % V: 55 %
Mordant et al., (2011)[51]	500 - 650 nm 300 wavebands	ϵ , S	OS, d, c, η	A: 104 % V: 35 %
Salyer et al., (2006)[52]	420 – 700 nm 29 wavebands	ϵ	OS, S	Arterial OS correlated well with <i>ex vivo</i> blood OS measurements
Khoobei et al., (2007)[53]	522 – 586 nm 7 wavebands	ϵ	OS	A: 92 % V: 76 %
Arimoto et al., (2010)[54]	510 – 600 nm 45 wavebands	ϵ	OS	N/A: relative OS
Furukawa et al., (2012)[54]	510 – 600 nm 7 wavebands	ϵ	OS	N/A: relative OS
Gao et al., (2012)[44]	510 - 586 nm 8 wavebands	ϵ	OS	N/A: relative OS

189
190
191
192
193

Key: A = arteries, V = veins. SO_2 = oxygen saturation, ϵ = extinction coefficient of Hb and O_2Hb , ϵ_{mel} = extinction coefficient of melanin, S = scattering contribution; c = concentration of haemoglobin, η = single/double pass contribution factor; d = diameter of vessels; K = contrast reduction factor.

194

195 **3. BLOOD VESSELS TARGETED FOR OXIMETRY**

196 **3.1. Retinal oximetry**

197 To date, the retinal vasculature has been the primary target for oximetry investigations in the eye.
198 The retina is a site of extremely high metabolic demand, and problems with retinal blood flow can
199 lead to a number of serious ocular conditions, including: retinal vascular occlusion[23–26] and diabetic
200 retinopathy.[13–17] Further, in ocular conditions characterised by cell loss e.g. glaucoma, estimation
201 of oxygen utilisation has provided new insights.[18–22]

202 **Choroidal oximetry**

203 A recent development in oximetry is the targeting of choroidal vessels for oximetry in subjects with
204 very low retinal pigmentation. The lack of retinal pigmentation allows light to traverse through the
205 retina and and dense choroidal vasculature. Kristjansdottir et al., (2013)[28] conducted an imaging
206 study of OS of choroidal blood vessels in healthy subjects; results were reported in terms of ODR
207 because ODR to OS calibration coefficients for choroidal vessels are not known and high levels optical
208 scattering prevent the use of existing oximetry models. For example, some choroidal vessels have a
209 negative optical density; i.e. they appear brighter than surrounding tissue. To date, a calibration
210 scheme for choroidal oximetry calibration has not been derived. However, this study revealed a very
211 low artery-vein difference of 4% in the choroid (instead of the typical ~30% artery-vein difference in
212 retinal vessels).[11,28] Further studies of the choroidal circulation are required to understand what
213 further physiological and clinical insights choroidal oximetry could bring.

214 **3.2. Bulbar conjunctival oximetry**

215 A recent oximetry study by MacKenzie et al., (2016)[32] revealed that bulbar conjunctival blood
216 vessels have oxygen dynamics that are remarkably different from any other blood vessels in the eye.
217 The bulbar conjunctival blood vessels are situated within the thin conjunctival membrane on the outer
218 surface of the sclera, and consequently are in direct contact with ambient air. This unique position of
219 the bulbar conjunctival vessels leads to oxygen diffusion occurring from air into the bulbar conjunctival
220 blood vessels. Consequently, all bulbar conjunctival blood vessels exposed to air will be highly
221 oxygenated, with little to no artery-vein difference. Study of bulbar conjunctival oxygen dynamics
222 could potentially yield insights into microvascular oxygen dynamics and related parameters. This may
223 be of particular interest for the study of oxygen dynamics in diabetes, where microvascular vessel wall
224 hardening is known to occur.[32]

225 **3.3. Episcleral oximetry**

226 Oximetry of the superficial episcleral blood vessels embedded into the sclera has recently been
227 achieved for the first time by MacKenzie et al (2016).[32] This study observed that when episcleral
228 vessels are exposed to a temporary hypoxic intervention, episcleral vessels dilated and episcleral OS
229 decreased. This auto-regulatory behaviour is similar to the autoregulation observed in retinal vessels
230 under similar hypoxic conditions.[11] Because episcleral vessels can be imaged on the surface of the
231 sclera, it has been suggested that episcleral vessels could be used as a proxy for retinal OS in situations
232 where retinal imaging is not feasible; e.g. in patients with cataracts. Alternatively, episcleral vessels
233 could be used as a comparison point with retinal vessels to study ocular autoregulation. Further

234 studies of episcleral vessels is required before their utility for clinically relevant oximetry can be
235 ascertained.[32]

236 **3.4. Oximetry elsewhere in the body**

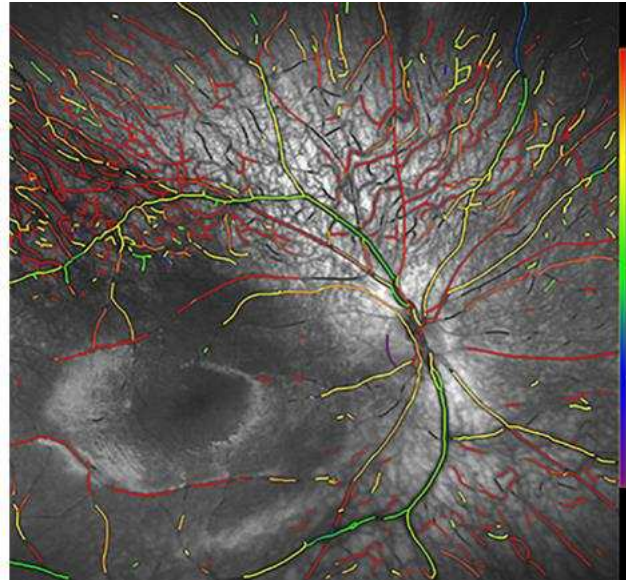
237 It is noteworthy that oximetry techniques originally developed for oximetry in the eye have
238 benefited oximetry applications elsewhere in the body. For example, multispectral imaging oximetry
239 has been employed to investigate diverse applications, including murine brain vascular oximetry,[55]
240 diabetic foot-ulcer development,[56] bowel laparoscopy,[57] skin blood flow,[58] the study of skin
241 damage due to beta radiation exposure,[59] labial, periodontal, and sublingual microvasculature,[60]
242 cancer tumour development in murine models,[39,40] and oximetry of the rat spinal cord dorsal vein
243 for studying the development of multiple sclerosis disease models.[38]

244 **4. SPECTROSCOPIC IMAGING MODALITIES FOR THE EYE**

245 The majority of oximetry studies in the eye are conducted with retinal-fundus cameras adapted for
246 two wavelength or multispectral imaging. Dual wavelength imaging can be enabled by splitting a
247 broadband retinal image with a dichroic beam-splitter, spectrally filtering the resultant images, and
248 then recording with one or more detectors.[4,31] Alternatively, wavebands may be recorded using
249 separate channels of a three-colour RGB CCD detector with additional spectral filtering to enhance
250 spectral discrimination.[9,38] The majority of multispectral and hyperspectral imaging studies have
251 employed time-sequential filtering of broadband retinal images, utilising either multiple bandpass
252 filters, a liquid-crystal tuneable filter (LCTF),[21,50,51,53,61,62] or an acousto-optic tuneable filter
253 (AOTF) for spectral discrimination.[54,63,64] LCTFs and AOTFs offer the advantages electronically-
254 controlled optical waveband switching in short timescales (~ 50 ms and 25 μ s respectively), with a
255 wide-variety of accessible wavelengths.[65] The Image Replicating Imaging Spectrometer (IRIS) has
256 enabled video-rate oximetry which has been utilised observe oxygen release by *ex vivo* red blood cells
257 upon exposure to sodium dithionite.[46,66]

258
259 Dual-wavelength scanning laser ophthalmoscopes (SLOs)[10,29,67,68] offer several advantages for
260 retinal oximetry compared to fundus cameras, including improved control of stray light, reduced
261 fundus light exposure levels, wide-field retinal scanning,[10] no requirement for pupil dilation,[68] and
262 the option to incorporate adaptive optics to compensate for eye motion and improve imaging of small
263 retinal blood vessels.[29] Recently this has enabled retinal oximetry of infants without mydriasis.⁵²
264 However, despite these advantages, SLOs are limited to available laser wavelengths, which are not
265 optimal for oximetry,[33] so further development and testing of SLO oximetry systems is required.

266
267 Slit lamps have not yet been utilised for oximetry, but could be modified for multispectral imaging.
268 The high magnification and resolution of slit lamps could enable oximetry of blood vessels as small as
269 individual capillaries and groups of red blood cells in the bulbar conjunctiva.[27]



270

271 **Figure 3.** Psuedo-colour OS map of retinal vessels in an infant obtained via imaging with
272 a scanning laser ophthalmoscope. Red indicates 100% OS, purple 0% OS. Figure
273 reproduced from Vehmeijer et al., (2016) under a Creative Commons BY license[68]

274 Optical Coherence Tomography (OCT) is emerging as a potential retinal oximetry technology, but
275 to date OCT oximetry has been applied only to murine models. In OCT, light backscattered from tissue
276 is collected, and by coherence gating, is processed to form a 3D volumetric image of tissue. The ranging
277 function of OCT provides the enhanced possibility of good control of the light paths defining optical
278 absorption and with a reduced influence of scattering Spectroscopic Optical Coherence Tomography
279 (S-OCT) has recently emerged as technology capable of recording 3D maps of OS with high spatial
280 resolution. [69–71] Initially, S-OCT systems utilised the near infra-red illumination wavelengths
281 commonly used by OCT systems. Unfortunately, near infra-red wavelengths suffer from weak optical
282 absorption contrast between Hb and O₂Hb, resulting in sub-optimal oximetry. Consequently, newer S-
283 OCT oximetry systems have improved oximetry capability by switching to visible wavelength
284 illumination; visible wavelengths provide improved spectral contrast for oximetry. [72,73] However,
285 S-OCT requires long acquisition times of up to 20 minutes for data acquisition. As such S-OCT oximetry
286 studies have been conducted in murine models only. [74–76]

287 Photoacoustic imaging has recently emerged as a hybrid imaging modality that combines optical
288 spectral contrast with the tissue depth penetration of ultrasound. In photoacoustic imaging, high
289 intensity pulsed laser light (typically < 10 ns duration per pulse) is incident on the target tissue, heating
290 the blood by less than 0.1°C and leading to rapid expansion and contraction which generates an
291 ultrasound pulse with an amplitude proportional to the absorption of light by blood.[77] Ultrasound
292 imaging of the emission therefore enables deep-tissue volumetric mapping of optical absorption.
293 However, the high laser powers required for photoacoustic signal generation and requirement for
294 ultrasonic transducer coupling to the eye make photoacoustic imaging a less attractive prospect for
295 oximetry in the human eye compared to oximetry with fundus cameras. So far all photoacoustic
296 studies of the eye have been limited to murine models. A good overview of photoacoustic ophthalmic
297 imaging has been provided by Liu and Zhang (2016).[78]

298

299 5. VALIDATION AND TESTING OF OXIMETRY MEASUREMENTS

300 5.1 Oxygen-sensitive challenges and interventions

301 Oxygen-sensitive physiological challenges and interventions alter OS in subjects, allowing the
302 oximetry capability of measurement systems to be assessed, and to provide useful calibration points
303 for oximetry.[1,3,31,38,74] Further, these challenges and interventions provide physiological insights
304 into metabolism.

305 5.1.1. Hyperoxia

306 Perhaps the most commonly used oxygen sensitive intervention is short duration hyperoxia (i.e. an
307 excess of O₂), where a subject breathes a high O₂ (typically 100% O₂) air mixture. Hyperoxia greatly
308 increases the partial pressure of oxygen (pO₂) in blood and increases both venous and arterial OS.

309 Using the *Oxymap* system, Hardarson et al., (2006)[4] reported that retinal arterial OS is increased
310 from 96 ± 9% OS (mean ± SD) at normoxia to 101 ± 8 % OS at hyperoxia. Retinal veins experience a
311 greater increase in OS from 55 ± 14 % to 78 ± 15%.[4] Using the *Imedos* system, Hammer et al.,
312 (2008)[9] reported that retinal arterial OS increased from 98 ± 10% (mean ± SD) at normoxia to 100
313 ± 10 % at hyperoxia and that retinal venous OS increased from 65 ± 12% at normoxia to 72 ± 10 % at
314 hyperoxia.[9] Also using the *Oxymap* system, Klefter et al., (2014)[79] reported that retinal arterial OS
315 increased from 95.1 ± 5.0% (mean ± SD) at normoxia to 96.6 ± 6.4% at hyperoxia and that retinal
316 venous OS increased from 62.9 ± 6.7% at normoxia to 70.3 ± 7.8% at hyperoxia. Notably retinal and
317 veins constricted in diameter by 5.5% and 8.2%, respectively at hyperoxia compared with normoxia.
318 In all cases the increase in retinal venous OS was greater than the increase in retinal arterial OS.

319 A hyperoxia intervention was used by Krisjandottir et al., (2013)[28] to show that all choroidal
320 vessels are highly oxygenated at normoxia; this could only have been achieved with a hyperoxia
321 intervention because two-wavelength oximetry calibration has not yet been demonstrated for
322 choroidal vessels.[28]

323 5.1.2. Hypoxia

324 An alternative OS-sensitive intervention is acute mild hypoxia, where systematic OS is decreased
325 by subjects inhaling a hypoxic air mixture (typically ~ 15% O₂) for several minutes. The 10 - 15 % OS
326 decrease induced by acute mild hypoxia studies is similar in magnitude to the decrease in OS
327 experience in high-altitude airplane travel [80] and thus can be considered safe in healthy subjects for
328 short durations.

329 Choudhary et al., (2013)[11] investigated the auto-regulatory effects of acute mild hypoxia in
330 retinal vessels. OS was observed to decrease for both arterioles and venules but artery-vein (AV) OS
331 difference remained constant. Both retinal arteries and veins were observed to dilate under hypoxia,
332 with arteries showing a larger increase.[11] This provided new insight into the interplay between the
333 vascular and choroidal oxygen supplies in the retina and auto-regulatory responses.

334 MacKenzie et al., (2016)[32] utilised a similar hypoxia intervention to study bulbar conjunctival and
335 episcleral oxygen dynamics. Episcleral vessels were observed to behave similarly to retinal vessels
336 under acute mild hypoxia, but episcleral arteries and veins were not distinguished. However, hypoxic
337 bulbar conjunctival vessels were observed to re-oxygenate to high OS via oxygen diffusion when

338 exposed to ambient air. This effect would not have been possible to observe without the hypoxic
339 intervention.[32]

340 Severe graded hypoxia to as low as 9% O₂ was used by Yi et al., (2015)[74] to investigate the
341 metabolic response of the rat retina to hypoxia, finding that the metabolic demand of the retina is
342 increased at hypoxia.[74]

343 5.1.3. Retinal light exposure

344 Retinal light exposure is known to alter retinal metabolic demand, thus inducing an autoregulation
345 effect, and thus altering retinal OS. Using the *Oxymap* system, Hardarson et al., (2009)[8] found that
346 retinal OS of both arteries and veins is higher in for an eye not exposed to light than for an eye exposed
347 to light.[8] With the *Imedos* system, Hammer et al., (2011)[6] found that retinal venous OS increased
348 by an average of ~ 5% after ~ 100s of 12.5 Hz flicker stimulation. In contrast, retinal arterial OS
349 decreased slightly on average by ~ 1%. The diameter of both arteries and veins increased significantly,
350 indicating increased blood flow. A later study by Hammer et al., (2012)[7] that compared diabetic
351 patients to healthy controls found that venous OS of diabetic patients increased less under flicker
352 stimulation than the change observed in healthy controls.[7] Similarly, venous dilation was less for
353 diabetic patients than healthy controls. This suggests that retinal blood flow regulation is impaired in
354 diabetic patients.[7]

355 5.2. Eye-mimicking *ex vivo* oximetry phantoms

356 Oximetry can be validated using *ex vivo* blood of various OS levels in *in vitro* phantoms that mimic
357 blood vessels within the eye. Various strategies to phantom design and construction have been
358 implemented.

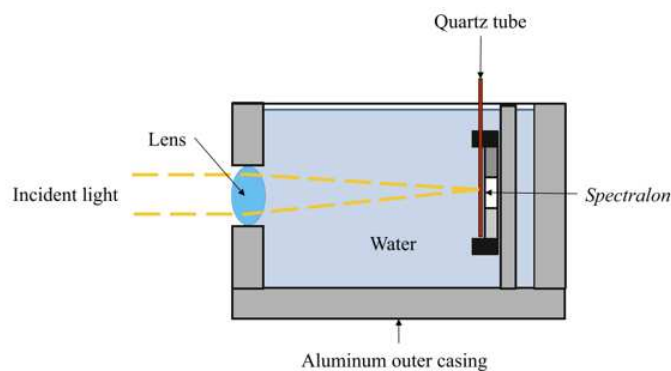
359 Lemaillet et al., (2009)[81] developed a multi-layered dynamic eye phantom, incorporating flowing
360 blood to simulate *in vivo* blood flow. Flowing blood is known to have different reflectance and
361 scattering parameters than static blood due to alignment of red blood cells in laminar flow
362 conditions.[82,83] The phantom consisted of: a plano-convex lens to mimic the human lens, a choroid
363 mimicking layer, and a layer mimicking the retinal pigment endothelium. A 100 µm capillary was
364 supplied with flowing bovine blood from a reservoir, and OS was modified by adding sodium
365 hydrosulphide to deoxygenate blood, with additional oxygen supplied via a fuel cell to the blood
366 reservoir. It was noted that construction of this phantom was highly time consuming.[81]

367 Mordant et al., (2011)[62] constructed a simple model eye consisting of straight quartz capillaries
368 of various inner diameters (50, 100, and 150 µm) filled with static human blood (see Figure 4). A convex
369 lens mimicked the human lens and distilled water mimicked the vitreous humour. A white diffuse
370 reflectance material - *Spectralon*[™] - mimicked the scleral back-reflectance.[30,84] Blood OS was varied
371 by placing samples in air mixtures with varied fractions of O₂ and OS was confirmed with a blood gas
372 analyser.[62] This phantom was used to validate later *in vivo* oximetry studies.[51]

373 MacKenzie et al., (2016)[32] constructed a simple sclera-mimicking phantom for bulbar
374 conjunctival and episcleral oximetry. This phantom consisted of a 100 µm FEP plastic capillary above
375 a *Spectralon*[™] backing. The capillary was filled with flowing *ex vivo* equine blood and OS was varied by
376 addition of sodium dithionite[66]; OS was confirmed with a blood gas analyser. Whilst not
377 sophisticated, this phantom was sufficient for oximetry validation.[32]

378 Recently, Ghassemi et al., (2015)[85,86] have reported a bio-mimicking phantom designed from
379 real retinal blood vessel patterns. These phantoms are 3D printed from a photoreactive resin in a
380 pattern based up a 3D sectioned image of retinal vessels. A commercially available O₂Hb solution was
381 used in place of whole blood. Yeast was used to consume oxygen in the solution, with OS decreasing
382 over time.[85] Bio-mimicking phantoms may be advantageous in future because they could simulate
383 realistic blood flow patterns and thus reproduce features like laminar flow seen in branching retinal
384 veins.[42]

385 Corcoran et al., (2014)[87] created an advanced, wide-field spherical eye with 3D-printed phantom
386 retina, an optics based on a rigorous schematic eye model. The retina incorporated embedded image
387 resolution test targets and simulated retinal tissue layers. This style of advanced phantom has not yet
388 been applied to oximetry, but could be highly beneficial in future studies that more closely resemble
389 *in vivo* applications.[87]



390

391 **Figure 4.** Diagram of a model eye phantom used by Mordant et al., (2011)[62] to validate
392 oximetry capability of a hyperspectral imaging system. Figure reproduced with
393 permission.

394 6. CLINICAL INSIGHTS

395

396 6.1. Diabetic retinopathy

397

398 Diabetic retinopathy is an important potentially blinding eye condition, which can affect patients
399 in the working-age population. Diabetic retinopathy causes loss of capillaries in the retinal circulation,
400 and visual loss can occur following the resultant retinal ischaemia, production of vaso-proliferative
401 substances e.g. vascular endothelial growth factor (VEGF), and then misdirected growth of new
402 vessels, which are fragile, and ultimately result in vitreous haemorrhage and/or retinal detachment.
403 Diabetic visual loss can also follow leakage from retinal vessels close to the macula causing macular
404 oedema. Research has explored the use of retinal oximetry to detect the effects on arterial and venous
405 oxygen saturation of diabetic retinopathy. Early work by Beach et al. detailed acute changes in retinal
406 oxygen utilisation with hyperglycaemia.[13] Later work, using dual-wavelength oximetry has
407 demonstrated that higher venous oxygen saturation is associated with established diabetic
408 retinopathy,[17] which, in some studies shows a dose-related relationship with increasing severity of
409 proliferative diabetic retinopathy.[15,16] These observations might represent the formation of
410 arterio-venous shunts in the retinal circulation to circumvent the capillary loss, or, alternatively, might

411 simply represent reduced oxygen utilisation by pathologically atrophic inner retinal cellular elements.
412 Elevated venous saturation in patients with diabetic retinopathy may be a clinically useful measure of
413 underlying retinal ischaemia, and may become an indicator of the need for retinal photocoagulation
414 treatment. Interestingly, application of retinal photocoagulation has not been shown to result in any
415 significant changes in venous retinal OS.[15]
416

417 **6.2. Retinal vessel occlusion**

418

419 Retinal venous occlusion is an important cause of visual morbidity in older patients with general
420 vascular risk factors, e.g. hypertension. The pathological effects of a central retinal vein occlusion may
421 include retinal ischaemia, production of VEGF, and growth of new vessels, which can cause visual loss
422 from vitreous haemorrhage, or neo-vascular glaucoma. Retinal oximetry research has been directed
423 at detecting OS abnormalities. Such abnormalities might provide early evidence of retinal ischemia,
424 and thus enable treatment to be applied at an earlier stage; hopefully reducing the risk of the patient
425 developing neo-vascular glaucoma. Dual-wavelength oximetry research studies in central retinal
426 venous occlusion have consistently shown lower levels of venous OS, consistent with generalised
427 retinal ischaemia.[24, 25] Studies in partial, or branch, retinal occlusion have shown variable results,
428 with sometimes increased, and sometimes reduced venous saturations. This may reflect the different,
429 localised impact of a venous occlusion, and/or the maturity of the occlusion, as well as the impact of
430 local homeostatic mechanisms.[23,26] Central retinal artery occlusion has been noted to result in
431 severe retinal hypoxia, with low arteriovenous difference, suggesting cell death.

432

433 **6.3. Glaucoma**

434

435 Glaucoma is a common cause of blindness in older patients, and a family history of glaucoma is an
436 important risk factor. The diagnosis of glaucoma rests on detection of characteristic changes at the
437 optic nerve head which are associated with visual field loss. Many, but not all, patients with glaucoma
438 will have elevated intraocular pressure. The pathological change, which ultimately results in visual loss
439 is retinal ganglion cell axon loss, which essentially results in atrophy of the cellular elements of the
440 inner retina. Oximetry studies have investigated the changes in oxygen consumption within the retinal
441 circulation that are associated with the cellular loss. Research work using both dual wavelength and
442 multispectral imaging has demonstrated elevated venous saturation, with some studies showing
443 increasingly elevated venous saturation in more severely affected eyes.[18–22] These studies suggest
444 a role for retinal oximetry as a means to estimate inner retinal oxygen consumption in glaucoma and
445 other optic neuropathies. Further research is required to investigate whether interventions to lower
446 the intraocular pressure might demonstrate reversible changes in oxygen utilisation, which could be
447 a favourable prognostic outcome from the intervention.

448

449 **7. EXPERT COMMENTARY**

450 Oximetry in the eye has revealed a great deal about physiological norms and autoregulation in the
451 retina. However, there is still considerable insight to be gleaned in application of oximetry to choroidal,
452 episcleral, and bulbar conjunctival blood vessels. OS norms of these vessel beds require further study,
453 and may provide insights into disease development and treatment.

454

455 The advent of commercially available retinal oximetry systems, i.e. the *Oxymap* and *Imedos*
456 systems have enabled retinal oximetry in the clinic, which has allowed studies of many retinal diseases
457 with increasing statistical power. Clinical studies hold the potential to provide deeper insight into
458 disease development and treatment of conditions such as diabetic retinopathy,[13–17] glaucoma,[18–
459 22] and retinal vessel occlusion.[23–26]

460
461 The use of oxygen-sensitive interventions such as hyperoxia, hypoxia, and retinal light exposure
462 have been able to compliment oximetry measurements on provide comparative intervention tests. In
463 the retina a flicker intervention has enabled comparisons of the metabolic response of healthy control
464 subjects and patients with diabetic retinopathy.[6] Notably, oxygen-sensitive interventions have
465 enabled insight into the fundamental physiology of oxygen supply to the choroidal vessels,[28]
466 episcleral circulation, and bulbar conjunctival circulation.[27] There is much potential in investigating
467 these new targets for oximetry.

468
469 The development of new technology and innovation in image processing is also helping to drive
470 new oximetry applications that were not previously possible. With improved techniques, oximetry is
471 now possible in small retinal vessels,[29] in the choroid,[28] in the episcleral and bulbar conjunctival
472 vessels,[32] and in the retina of infants.[68] New applications will invariably find new insights into the
473 eye which are fundamentally and clinically important.

474
475 One of the fundamental challenges for oximetry is validation of measurements. Arterial OS can be
476 compared to invasive blood gas measurements or pulse oximetry. However, venous calibration is
477 extremely challenging, and is influenced by blood vessel diameter and fundus pigmentation.[9,31]
478 Multispectral algorithms offer a ‘calibration free’ oximetry method, but accurate validation is still
479 highly challenging due to the complex optical environment of the eye. Validation with *ex vivo* blood is
480 also complicated by numerous factors including blood aggregation, red blood cell death, alignment of
481 red blood cells under flow, and imperfect phantoms.[12,51,81]

482

483 **Five-year view**

484 In the last five years, oximetry has revealed the fundamental physiology of OS in episcleral
485 vessels,[27] the bulbar conjunctival vessels,[27] and the choroidal circulation.[28] The physiology
486 understanding of these vessel beds has been enabled by the development of hyperoxia and hypoxia
487 OS-sensitive interventions.

488 Application of oximetry to the eye is continuing to yield fresh insight into the physiology of the eye
489 and ocular disease development, and treatment. Commercially available two-wavelength oximetry
490 systems have enabled oximetry in the clinic and studies of diseases such as diabetic retinopathy, vessel
491 occlusion, and glaucoma have resulted. In the next five years, oximetry will likely be applied to
492 increasingly diverse disease applications.

493 Imaging technology and imaging analysis is also continuing to develop, pushing new boundaries in
494 spatial and temporal resolution. This can enable oximetry in new applications, such as the study of
495 small retinal vessels,[29] oximetry in infants,[68] in *ex vivo* red blood cells.[46] The advent of 3D
496 printing has allowed the development of bio-mimicking phantoms[87] based on real blood vessel

497 network patterns,[85] enabling the study of blood flow in realistic yet controlled scenarios. The fast
498 paced development of 3D printing makes this field of phantom development particularly promising.

499 **Key issues**

- 500 ▪ Spectroscopic oximetry is most widely applied to the study of the retinal circulation, but
501 oximetry of the bulbar conjunctival, episcleral, and choroidal circulations has also recently
502 emerged.
- 503 ▪ Oxygen-sensitive interventions such as hyperoxia, hypoxia, and retinal flicker illumination
504 provide oximetry validation, clinical insights, and have revealed fundamental physiology of
505 the choroid, the episcleral vessels, and the bulbar conjunctival vessels.
- 506 ▪ Commercial oximetry systems have enabled clinical studies in individual patients and in larger
507 group studies, enabling deeper understanding of the development and treatment of diseases
508 such as diabetes, retinal vessel occlusion, and glaucoma.
- 509 ▪ Development of new imaging capabilities, advanced image processing concepts, and ever-
510 improving phantom development are continuing to push new oximetry applications and
511 enable fresh insights into the physiology of the eye.

512

513 **7. CONCLUSIONS**

514 Oximetry has enabled many insights in the fundamental physiology and oxygen dynamics of the
515 eye. In particular, oximetry has enabled the study of retinal autoregulation, retinal disease
516 development, and retinal disease treatment. Recently, the fundamental oxygen dynamics of the
517 bulbar conjunctiva, the episcleral vessels, and the choroid have been revealed by oximetry combined
518 with complimentary OS-sensitive hyperoxia and hypoxia interventions.

519 Commercially available retinal oximetry systems have enabled oximetry in the clinic, allowing
520 studies of retinal OS in many diseases and treatments. In particular, diabetic retinopathy, retinal
521 vascular occlusion, and glaucoma. Oxygen sensitive interventions - such as retinal flicker illumination,
522 hypoxia, and hyperoxia - have provided means to validate oximetry, establish physiological norms,
523 and probe auto-regulation responses.

524 The predominant imaging systems in the field of retinal oximetry are based upon modified retinal-
525 fundus cameras, however SLO-based systems show considerable promise with a comparatively larger
526 field of view, the potential for improved spatial and depth resolution and accuracy. Further, SLOs
527 require no mydriasis. Yet, existing SLO systems are limited to commercially favoured laser
528 wavelengths, and as such may provide sub-optimal oximetry measurements. Confocal SLOs offer
529 potential for improved accuracy through improved control of stray light and the longer effect path
530 lengths enable good oximetric contrast with a wide range of low-cost infrared lasers, although optical
531 efficiency is necessarily lower. Further development of SLO oximetry systems is a particularly fertile
532 area.

533 New oximetry applications are currently emerging, namely oximetry of the small retinal vessels,
534 retinal oximetry in infants, and oximetry of the bulbar conjunctiva, episcleral, and choroidal vessels.
535 These new applications for oximetry will enable researchers to understand the OS in physiological
536 norms and disease across multiple ocular blood vessel beds.

537

538 **BIBLIOGRAPHY**

- 539 1. Hickam JB, Sieker HO, Frayser R. Studies of retinal circulation and A-V oxygen difference in man.
540 *Trans. Am. Clin. Climatol. Assoc.* 71(657), 34–44 (1959).
- 541 2. Hickam JB, Frayser R, Ross JC. A study of retinal venous blood oxygen saturation in human
542 subjects by photographic means. *Circulation.* 27(3), 375–385 (1963).
- 543 3. Hickam JB, Frayser R. Studies of the retinal circulation in man. Observations on vessel diameter,
544 arteriovenous oxygen difference, and mean circulation time. *Circulation.* XXXIII(February),
545 302–316 (1966).
- 546 4. Hardarson SH, Harris A, Karlsson RA, *et al.* Automatic retinal oximetry. *Invest. Ophthalmol. Vis. Sci.*
547 47(11), 5011–6 (2006).
- 548 5. Beach J. Pathway to retinal oximetry. *Transl Vis Sci Technol.* 3(5), 1–9 (2014).
- 549 6. Hammer M, Vilser W, Riemer T, *et al.* Retinal venous oxygen saturation increases by flicker light
550 stimulation. *Invest. Ophthalmol. Vis. Sci.* 52(1), 274–7 (2011).
- 551 7. Hammer M, Heller T, Jentsch S, *et al.* Retinal vessel oxygen saturation under flicker light
552 stimulation in patients with nonproliferative diabetic retinopathy. *Invest. Ophthalmol. Vis. Sci.*
553 53(7), 4063–8 (2012).
- 554 8. Hardarson SH, Basit S, Jonsdottir TE, *et al.* Oxygen saturation in human retinal vessels is higher
555 in dark than in light. *Invest. Ophthalmol. Vis. Sci.* 50(5), 2308–11 (2009).
- 556 9. Hammer M, Vilser W, Riemer T, Schweitzer D. Retinal vessel oximetry-calibration,
557 compensation for vessel diameter and fundus pigmentation, and reproducibility. 13(5), 1–7
558 (2008).
- 559 10. Kristjansdottir JV, Hardarson SH, Halldorsson GH, Karlsson RA, Eliasdottir TS, Stefánsson E.
560 Retinal oximetry with a scanning laser ophthalmoscope. *Investig. Ophthalmology Vis. Sci.* 55(5),
561 3120 (2014).
- 562 11. Choudhary TR, Ball D, Fernandez Ramos J, McNaught AI, Harvey AR. Assessment of acute mild
563 hypoxia on retinal oxygen saturation using snapshot retinal oximetry. *Invest. Ophthalmol. Vis. Sci.*
564 54(12), 38–43 (2013).
- 565 12. MacKenzie LE. Oximetry of bulbar conjunctival and episcleral microvasculature using snapshot
566 multispectral imaging. *Retin. Oximetry Work.* 2016. (2016).
- 567 13. Tiedeman JS, Kirk SE, Srinivas S, Beach JM. Retinal oxygen consumption during hyperglycemia
568 in patients with diabetes without retinopathy. *Ophthalmology.* 105(1), 31–36 (1998).
- 569 14. Jørgensen CM, Hardarson SH, Bek T. The oxygen saturation in retinal vessels from diabetic
570 patients depends on the severity and type of vision-threatening retinopathy. *Acta Ophthalmol.*
571 92(1), 34–39 (2014).
- 572 15. Jørgensen C, Bek T. Increasing oxygen saturation in larger retinal vessels after
573 photocoagulation for diabetic retinopathy. *Investig. Ophthalmol. Vis. Sci.* 55(8), 5365–5369
574 (2014).
- 575 16. Hammer M, Vilser W, Riemer T, *et al.* Diabetic patients with retinopathy show increased retinal
576 venous oxygen saturation. *Graefes Arch. Clin. Exp. Ophthalmol.* 247(8), 1025–30 (2009).
- 577 17. Hardarson SH, Stefánsson E. Retinal oxygen saturation is altered in diabetic retinopathy. *Br. J.*
578 *Ophthalmol.* 96(4), 560–3 (2012).

- 579 18. Olafsdottir OB, Hardarson SH, Gottfredsdottir MS, Harris A, Stefánsson E. Retinal oximetry in
580 primary open-angle glaucoma. *Invest. Ophthalmol. Vis. Sci.* 52(9), 6409–13 (2011).
- 581 19. Olafsdottir, OB Vandewalle E, Abegão, Pinto L Geirsdottir A, De Clerck E, *et al.* Retinal oxygen
582 metabolism in healthy subjects and glaucoma patients. *Br. J. Ophthalmology.* 98(3), 329–33
583 (2014).
- 584 20. Vandewalle E, Pinto LA, Olafsdottir OB, *et al.* Oximetry in glaucoma: Correlation of metabolic
585 change with structural and functional damage. *Acta Ophthalmol.* 92(2), 105–110 (2014).
- 586 21. Mordant DJ, Al-Abboud I, Muyo G, Gorman A, Harvey AR, McNaught AI. Oxygen saturation
587 measurements of the retinal vasculature in treated asymmetrical primary open-angle
588 glaucoma using hyperspectral imaging. *Eye.* 28(10), 1190–200 (2014).
- 589 22. Boeckeaert J, Vandewalle E, Stalmans I. Oximetry: recent insights into retinal vasopathies and
590 glaucoma. *Bull. Soc. Belge Ophthalmol.* (319), 75–83 (2012).
- 591 23. Hardarson SH, Stefánsson E. Oxygen saturation in branch retinal vein occlusion. *Acta*
592 *Ophthalmol.* 90(5), 466–470 (2012).
- 593 24. Hardarson SH, Elfarsson A, Agnarsson BA, Stefansson E. Retinal oximetry in central retinal
594 artery occlusion. *Acta Ophthalmol.* 91(2), 189–190 (2013).
- 595 25. Eliasdottir TS, Bragason D, Hardarson SH, Kristjansdottir G, Stefánsson E. Venous oxygen
596 saturation is reduced and variable in central retinal vein occlusion. *Graefe's Arch. Clin. Exp.*
597 *Ophthalmol.* (2014).
- 598 26. Lin L-L, Dong Y-M, Zong Y, *et al.* Study of retinal vessel oxygen saturation in ischemic and non-
599 ischemic branch retinal vein occlusion. *Int. J. Ophthalmol.* 9(1), 99–107 (2016).
- 600 27. MacKenzie LE, Choudhary TR, McNaught AI, Harvey AR. In vivo oximetry of human bulbar
601 conjunctival and episcleral microvasculature using snapshot multispectral imaging. *Exp. Eye*
602 *Res.* 149, 48–58 (2016).
- 603 28. Kristjansdottir JV, Hardarson SH, Harvey AR, Olafsdottir OB, Eliasdottir TS, Stef E. Choroidal
604 oximetry with a noninvasive spectrophotometric oximeter. *Invest. Ophthalmol. Vis. Sci.* 54(5),
605 3234–3239 (2013).
- 606 29. Li H, Lu J, Shi G, Zhang Y. Measurement of oxygen saturation in small retinal vessels with
607 adaptive optics confocal scanning laser ophthalmoscopy. *JBO Lett.* 16(11) (2011).
- 608 30. Hammer M, Leistritz S, Leistritz L, Schweitzer D. Light paths in retinal vessel oxymetry. *IEEE*
609 *Trans. Biomed. Eng.* 48(5), 592–8 (2001).
- 610 31. Beach JM, Schwenzer KJ, Srinivas S, Kim D, Tiedeman JS. Oximetry of retinal vessels by dual-
611 wavelength imaging: calibration and influence of pigmentation. *JAP.* 86(2), 748–758 (1999).
- 612 32. MacKenzie LE, Choudhary TR, McNaught AI, Harvey AR. In vivo oximetry of human bulbar
613 conjunctival and episcleral microvasculature using snapshot multispectral imaging. *Exp. Eye*
614 *Res.* 149, 48–58 (2016).
- 615 33. Smith MH. Optimum wavelength combinations for retinal vessel oximetry. *Appl. Opt.* 38(1),
616 258–267 (1999).
- 617 34. Mackenzie LE. In vivo microvascular oximetry using multispectral imaging. Chapter 5: Rat spinal
618 cord oximetry. (November) (2016).
- 619 35. Pittman R, Duling B. A new method for the measurement of percent oxyhemoglobin. *J. Appl.*

- 620 *Physiol.* 38(2) (1975).
- 621 36. Delori FC. Noninvasive technique for oximetry of blood in retinal vessels. *Appl. Opt.* 27(6),
622 1113–1125 (1988).
- 623 37. Delori FC. Spectrophotometer for noninvasive measurement of intrinsic fluorescence and
624 reflectance of the ocular fundus. *Appl. Opt.* 33(31), 7439–7452 (1994).
- 625 38. van der Putten MA, MacKenzie LE, Davies AL, *et al.* A multispectral microscope for in vivo
626 oximetry of rat dorsal spinal cord vasculature. *Physiol. Meas.* (2016).
- 627 39. Sorg BS, Moeller BJ, Donovan O, Cao Y, Dewhirst MW. Hyperspectral imaging of hemoglobin
628 saturation in tumor microvasculature and tumor hypoxia development. *J. Biomed. Opt.* 10(4),
629 44004 (2005).
- 630 40. Sorg BS, Hardee ME, Agarwal N, Moeller BJ, Dewhirst MW. Spectral imaging facilitates
631 visualization and measurements of unstable and abnormal microvascular oxygen transport in
632 tumors. *J. Biomed. Opt.* 13(1), 14026 (2008).
- 633 41. Hammer M, Schweitzer D. Quantitative reflection spectroscopy at the human ocular fundus.
634 *Phys. Med. Biol.* 47(2), 179–91 (2002).
- 635 42. Hendargo HC, Zhao Y, Allenby T, Palmer GM. Snap-shot multispectral imaging of vascular
636 dynamics in a mouse window-chamber model. *Opt. Lett.* 40(14), 3292–3295 (2015).
- 637 43. Ramella-Roman JC, Mathews SA. Spectroscopic measurements of oxygen saturation in the
638 retina. *IEEE J. Sel. Top. Quantum Electron.* 13(6), 1697–1703 (2007).
- 639 44. Gao L, Smith RT, Tkaczyk TS. Snapshot hyperspectral retinal camera with the Image Mapping
640 Spectrometer (IMS). *Biomed. Opt. Express.* 3(1), 48–54 (2012).
- 641 45. Gorman AS. Snapshot spectral imaging using image replication and birefringent
642 interferometry: principles and applications. (2010).
- 643 46. Fernandez Ramos J, Brewer LR, Gorman A, Harvey AR. Video-rate multispectral imaging:
644 application to microscopy and macroscopy. In: *Classical Optics 2014, OSA Technical Digest.*
645 Optical Society of America, Washington, D.C. (2014).
- 646 47. Schweitzer D, Hammer M, Kraft J, Thamm E, Königsdörffer E, Strobel J. In vivo measurement of
647 the oxygen saturation of retinal vessels in healthy volunteers. *IEEE Trans. Biomed. Eng.* 46(12),
648 1454–65 (1999).
- 649 48. Drewes J, Smith M, Hiliman L, *et al.* Instrument for the measurement of retinal vessel oxygen
650 saturation. *BiOS'99 Int. Biomed. Opt. Symp. Int. Soc. Opt. Photonics.* 3591(January), 114–120
651 (1999).
- 652 49. Smith MH, Denninghoff KR, Lompando A, Hillman LW. Retinal vessel oximetry: toward absolute
653 calibration. *Proc. SPIE.* 3908, 217–226 (2000).
- 654 50. Alabboud I, Muyo G, Gorman A, *et al.* New spectral imaging techniques for blood oximetry in
655 the retina. *Proc. SPIE 6631, Nov. Opt. Instrum. Biomed. Appl. III.* 6631 (2007).
- 656 51. Mordant DJ, Al-Abboud I, Muyo G, *et al.* Spectral imaging of the retina. *Eye.* 25(3), 309–20
657 (2011).
- 658 52. Salyer DA, Beaudry N, Basavanthappa S, *et al.* Retinal oximetry using intravitreal illumination.
659 *Curr. Eye Res.* 31(7–8), 617–27 (2006).
- 660 53. Khoobehi B, Ning J, Puissegur E, Bordeaux K, Balasubramanian M, Beach J. Retinal oxygen

- 661 saturation evaluation by multi-spectral fundus imaging. 6511, 65110B–65110B–6 (2007).
- 662 54. Arimoto H, Furukawa H. Retinal oximetry with 510 - 600 nm light based on partial least-squares
663 regression technique. *Jpn. J. Appl. Phys.* 49(11) (2010).
- 664 55. Shonat RD, Wachman S. Near-simultaneous hemoglobin saturation and oxygen tension maps
665 in mouse brain using an AOTF microscope. *Biophys. J.* 73(September), 1223–1231 (1997).
- 666 56. Yudovsky D, Nouvong A, Schomacker K, Pilon L. Assessing diabetic foot ulcer development risk
667 with hyperspectral tissue oximetry. *J. Biomed. Opt.* 16(2), 26009 (2011).
- 668 57. Clancy NT, Arya S, Stoyanov D, Singh M, Hanna GB, Elson DS. Intraoperative measurement of
669 bowel oxygen saturation using a multispectral imaging laparoscope. *Biomed. Opt. Express.*
670 6(10), 4179–90 (2015).
- 671 58. Gupta N, Ramella-Roman JC. Detection of blood oxygen level by noninvasive passive spectral
672 imaging of skin. *Proc. SPIE.* 6842, 68420C–68420C–8 (2008).
- 673 59. Chin MS, Freniere BB, Lo Y-C, *et al.* Hyperspectral imaging for early detection of oxygenation
674 and perfusion changes in irradiated skin. *J. Biomed. Opt.* 17(2), 26010 (2012).
- 675 60. Townsend D, D’Aiuto F, Deanfield J. *In Vivo* Capillary Loop Hemoglobin Spectroscopy in Labial,
676 Sublingual, and Periodontal Tissues. *Microcirculation.* 22(6), 475–484 (2015).
- 677 61. Hirohara Y, Okawa Y, Mihashi T, *et al.* Validity of retinal oxygen saturation analysis:
678 hyperspectral imaging in visible wavelength with fundus camera and liquid crystal wavelength
679 tunable filter. *Opt. Rev.* 14(3), 151–158 (2007).
- 680 62. Mordant DJ, Al-Abboud I, Muyo G, *et al.* Validation of human whole blood oximetry, using a
681 hyperspectral fundus camera with a model eye. *Invest. Ophthalmol. Vis. Sci.* 52(5), 2851–9
682 (2011).
- 683 63. Furukawa H, Arimoto H, Shirai T, Ooto S, Hangai M, Yoshimura N. Oximetry of retinal capillaries
684 by multicomponent analysis. *Appl. Spectrosc.* 66(8), 962–969 (2012).
- 685 64. Patel SR, Flanagan JG, Shahidi AM, Sylvestre JP, Hudson C. A prototype hyperspectral system
686 with a tunable laser source for retinal vessel imaging. *Investig. Ophthalmol. Vis. Sci.* 54(8),
687 5163–5168 (2013).
- 688 65. Levenson R. Spectral imaging in biomedicine: A selective overview. *Proc. SPIE.* 3438, 300–312
689 (1998).
- 690 66. Briley-Saebo K, Bjornerud A. Accurate de-oxygenation of ex vivo whole blood using sodium
691 dithionite. *Proc. Intl. Soc. Mag. Reson. Med.* 8, 2025 (2000).
- 692 67. Ashman RA, Reinholz F, Eikelboom RH. Oximetry with a multiple wavelength SLO. *Int.*
693 *Ophthalmol.* 23(4–6), 343–346 (2001).
- 694 68. Vehmeijer WB, Magnúsdóttir V, Elíasdóttir TS, Hardarson SH, Schalijs-Delfos NE, Stefánsson E.
695 Retinal Oximetry with Scanning Laser Ophthalmoscope in Infants. *PLoS One.* 11(2), e0148077
696 (2016).
- 697 69. Faber DJ, van Leeuwen TG. Are quantitative attenuation measurements of blood by optical
698 coherence tomography feasible? *Opt. Lett.* 34(9), 1435–1437 (2009).
- 699 70. Lu C-W, Lee C-K, Tsai M-T, Wang Y-M, Yang CC. Measurement of the hemoglobin oxygen
700 saturation level with spectroscopic spectral-domain optical coherence tomography. *Opt. Lett.*
701 33(5), 416–8 (2008).

- 702 71. Kagemann L, Wollstein G, Wojtkowski M, *et al.* Spectral oximetry assessed with high-speed
703 ultra-high-resolution optical coherence tomography. *J. Biomed. Opt.* 12(4) (2007).
- 704 72. Robles FE, Chowdhury S, Wax A. Assessing hemoglobin concentration using spectroscopic
705 optical coherence tomography for feasibility of tissue diagnostics. *Biomed. Opt. Express.* 1(1),
706 310–317 (2010).
- 707 73. Yi J, Li X. Estimation of oxygen saturation from erythrocytes by high-resolution spectroscopic
708 optical coherence tomography. *Opt. Lett.* 35(12), 2094–6 (2010).
- 709 74. Yi J, Liu W, Chen S, *et al.* Visible light optical coherence tomography measures retinal oxygen
710 metabolic response to systemic oxygenation. *Light Sci. Appl.* 4(9), e334 (2015).
- 711 75. Chen S, Yi J, Zhang HF. Measuring oxygen saturation in retinal and choroidal circulations in rats
712 using visible light optical coherence tomography angiography. *Biomed. Opt. Express.* 6(8), 2840
713 (2015).
- 714 76. Chong SP, Merkle CW, Leahy C, Radhakrishnan H, Srinivasan VJ. Quantitative microvascular
715 hemoglobin mapping using visible light spectroscopic Optical Coherence Tomography. *Biomed.*
716 *Opt. Express.* 6(4), 1429 (2015).
- 717 77. Beard P. Biomedical photoacoustic imaging. *Interface Focus.* 1(4), 602–31 (2011).
- 718 78. Liu W, Zhang HF. Photoacoustic imaging of the eye : a mini review. *Biochem. Pharmacol.* (2016).
- 719 79. Klefter ON, Lauritsen AØ, Larsen M. Retinal hemodynamic oxygen reactivity assessed by
720 perfusion velocity, blood oximetry and vessel diameter measurements. *Acta Ophthalmol.* , 1–
721 10 (2014).
- 722 80. Humphreys S, Deyermond R, Bali I, Stevenson M, Fee JPH. The effect of high altitude
723 commercial air travel on oxygen saturation. *Anaesthesia.* 60(5), 458–60 (2005).
- 724 81. Lemaillot P, Ramella-Roman JC. Dynamic eye phantom for retinal oximetry measurements. *J.*
725 *Biomed. Opt.* 14(6) (2009).
- 726 82. Klose HJ, Volger E, Brechtelsbauer H, Heinich L, Schmid-Schönbein H. Microrheology and light
727 transmission of blood. *Pflügers Arch. - Eur. J. Physiol.* 333(2), 126–139 (1972).
- 728 83. Hammer M, Schweitzer D, Michel B, Thamm E, Kolb a. Single scattering by red blood cells.
729 *Appl. Opt.* 37(31), 7410–7418 (1998).
- 730 84. Rodmell PI, Crowe JA, Gorman A, *et al.* Light path-length distributions within the retina. *J.*
731 *Biomed. Opt.* 19(3), 36008 (2014).
- 732 85. Ghassemi P, Wang J, Melchiorri AJ, *et al.* Rapid prototyping of biomimetic vascular phantoms
733 for hyperspectral reflectance imaging. *J. Biomed. Opt.* 20(12), 121312 (2015).
- 734 86. Wang J, Ghassemi P, Melchiorri A, *et al.* 3D printed biomimetic vascular phantoms for
735 assessment of hyperspectral imaging systems. *Des. Perform. Valid. Phantoms Used Conjunction*
736 *with Opt. Meas. Tissue VII, Proc. SPIE.* 9325 (2015).
- 737 87. Corcoran A, Muyo G, van Hemert J, Gorman A, Harvey AR. Application of a wide-field phantom
738 eye for optical coherence tomography and reflectance imaging. *J. Mod. Opt.* 62(21), 1828–1838
739 (2015).

740 **Financial and competing interests**

741 The authors report no conflicts of interest.